

원자로압력용기강의 동적 응력확대계수와 동적 균열전파속도

이역섭*, 한민구**, 한문식***

Dynamic Stress Intensity Factor and Dynamic Crack Propagation Velocity in Nuclear Pressure Vessel Steels

O. S. Lee*, M. K. Han** and M. S. Han***

ABSTRACT

동적 파괴인성치 측정시스템과 동적 2차원 유한요소해석 프로그램을 개발하여 원자로압력용기에 사용하는 강(SA508 c1.3, SA516 gr.70)의 동적 파괴인성치와 동적 균열정지인성치를 평가하고 이에 대한 유용성을 확인하였으며, 이 시스템을 이용하여 재료의 동적 파괴특성을 규명하였다. SA508 c1.3와 SA516 gr.70의 동적 균열전파속도(\dot{a})에 대응하는 동적 응력확대계수($K(\dot{a})$)에 대한 실험식을 얻었으며, 동적 응력확대계수와 동적 균열전파속도와의 관계는 전형적인 "R"형으로 나타남을 확인하였다.

Key Words : Dynamic Stress Intensity Factor(동적응력확대계수), Dynamic Crack Propagation Velocity(동적균열전파속도), Nuclear Pressure Vessel Steels(원자로압력용기강), Dynamic Crack Arrest Toughness(동적균열정지인성값), Two-Dimensional Dynamic Crack Analysis Program(2차원 동적균열해석프로그램)

1. Introduction

Various defects exist in material. The growth pattern of cracks from these defects depends on the magnitude and applied condition of a load. Mechanical structure may be considered to be safe before cracks reach critical sizes. However, cracks smaller than critical sizes can propagate with very high speed(e.g. 1500m/s for steel) for some cases by unexpected impact loads(such as thermal impact or dynamic load impact). This

rapid propagation can cause hazardous accidents for nuclear pressure vessels.

With the support of EPRI and NRC (Nuclear Regulatory Commission), Battelle Research Center, MRL in The University of Maryland, and The University of Illinois at Urbana - Champaign have developed measuring methods for determining the crack arrest toughness of nuclear pressure vessel steels since 1976.

As a result, the measurement methods have been standardized to some degree.

* 인하대학교 기계공학과
** 거제대학 기계과
*** 계명대학교 자동차공학부

In Korea, much research has been done for it on static fracture mechanics and the propagation behavior of fatigue crack. However, only a few researchers such as Lee⁽¹⁾, Irwin et al⁽²⁻³⁾, Knauss et al⁽⁴⁾, Closley et al⁽⁵⁾, Lee and Han⁽⁶⁾ have carried out research on dynamic fracture characteristics of nuclear pressure vessel grade steels and high polymers. Lee and coworkers developed an equipment measuring dynamic crack propagation velocity and published a research paper on the reliability of the equipment⁽⁷⁾. They also carried out basic research on dynamic fracture characteristics of high polymers by using the dynamic optical-elastic experiment equipment in Inha University, which was installed for the first time in Korea with IBRD FUND. That is, they suggested the methodology for applying dynamic fracture mechanics to the development of new materials by systematically carrying out research on dynamic fracture parameters of several high polymers(such as polycarbonate, Homalite-100, PMMA, and Epoxy)⁽⁸⁾.

However, research on the dynamic fracture mechanics in Korea is still at the initial stage. Measuring methods of dynamic stress intensity factor and dynamic crack arrest toughness need to be further developed for materials of nuclear pressure vessels and large sized structures. Research on the application of the dynamic fracture mechanics should be also further made.

In this research, using INSAMCR(INha Stress Analysis of Moving CRacks), two-dimensional dynamic crack analysis program, we obtained dynamic stress intensity factors of nuclear pressure vessel steels(SA508 Cl.3 and SA516 gr.70) and identified various physical properties affecting these factors. We also proposed empirical equations correlating dynamic stress intensity factors with dynamic crack propagation velocities.

2. Experimental Method and Procedure

Figure 1 shows a procedure for automatically

determining dynamic fracture toughness. INSAMCR-MAIN Program of PULL-DOWN MENU type controls all experimental test/analysis system and a internal program for automatic procedure. The test/analysis system include a Universal Test Machine(for dynamic tension and compression test), a peripheral device(for storing data), a measuring equipment (for dynamic crack propagation velocity), a A/D converter, NISA II / DISPLAY III program(for static analysis with initial static test data), INSAMCR program(for analyz-

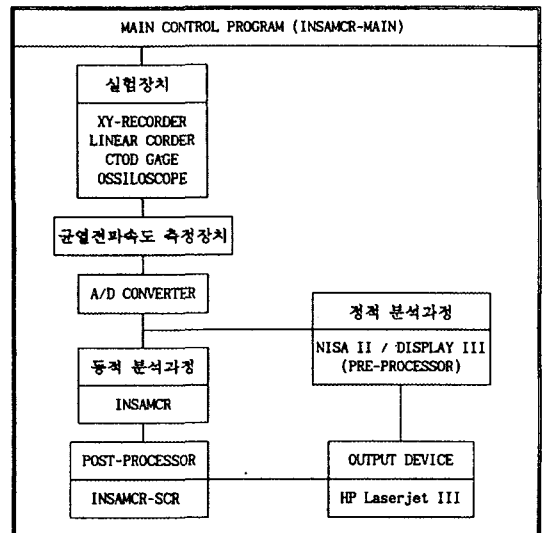


Fig. 1 Flow-Chart of Automatic Procedure for the Extraction of the Dynamic Fracture Toughness

Table 1. Mechanical Properties of Materials for Experiments.

Material	SA508 cl.3	SA516 gr.70
Modulus of elasticity (GPa)	204.0	202.0
Poisson's ratio	0.3	0.3
Elongation (%)	20.0	23.0
Yield stress (MPa)	344.7	397.3
Ultimate stress (MPa)	637.7	549.4
Density (Kg/m ³)	7850.0	7841.0

Table 2. Chemical Compositions of Materials for Experiments. (wt. %)

Materials	C	Si	Mn	P	S	Ni	Cr	Mo	V	Al	Cu
SA508 cl.3	0.20	0.06	1.44	0.007	0.004	0.82	0.150	0.54	0.003	0.006	0.04
SA516 gr.70	0.17	0.25	1.05	0.013	0.003	0.02	0.024	0.01	0.045	0.041	-

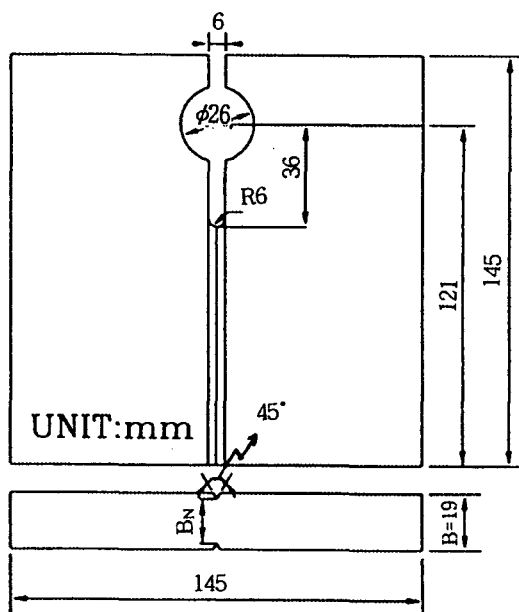


Fig. 2 Dimensions of CLWL Specimen

ing dynamic fracture toughness, dynamic crack arrest toughness and dynamic crack propagation behavior), INSAMCR-SCR program(for postprocessing data), and a HP Laserjet 4MV printer. In this research, we used specimens of SA 508 Cl.3 with a thickness of 20mm and SA 516 gr.70 with a thickness of 19mm which have been used widely for nuclear pressure vessels. The mechanical properties and chemical compositions of the specimens are shown in Tables 1 and 2, respectively. The geometric shape of a CLWL(Crack Line Wedge Loaded) specimen is shown in Fig.2.

As shown in Fig.3, test specimens were com-

pressed with a speed of 5mm/min by Universal Test Machine(Toyo Baldwin, 10ton, Japan) until the specimens were fractured. Eight Conductive Silver Paint Lines with a thickness of $1\text{mm} \pm 0.1\text{mm}$ were painted on the specimens at 4mm intervals from a crack tip parallel and perpendicularly in the propagation direction, respectively. The measuring equipment measured the dynamic crack propagation velocity of each specimen by processing the signals sent from the silver lines torn by the propagating crack. Since the test specimen in this research was conductive material, a thin paper was pasted on the surface of the specimen and then the paint lines are marked with adhesive masking tape. The thin paper on the surface was dry-hardened with about 200°C for 30 minutes to make the dynamic crack propagation property of the thin paper equal to that of the specimen. Nonconductive paint could be used instead of the thin paper. However, it was not used in this research because acetone used for painting silver paint lines could melt nonconductive paint, and the melted paint could be conducted to conductive mother material. Crack propagation gauge on U.S. market proved to be inappropriate for research on dynamic crack propagation behavior because the gauge was fractured in the direction different from the dynamic crack propagation direction.

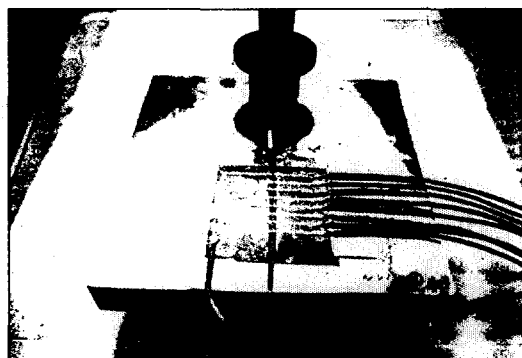


Fig. 3 Schematic Diagram of Wedge Loading Arrangement

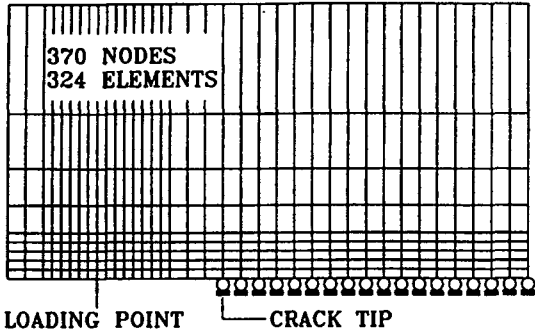


Fig. 4 Finite Element Mesh used to Model the Upper Half of the CLWL Specimen

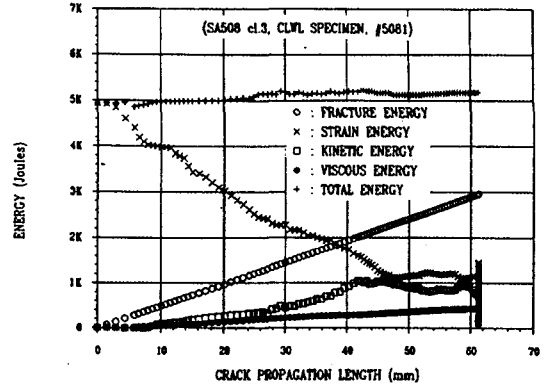
Figure 4 shows the finite element model of the CLWL specimen used in the experiment for the analysis by the finite element analysis program, INSAMCR.

3. Experimental Results (and Consideration)

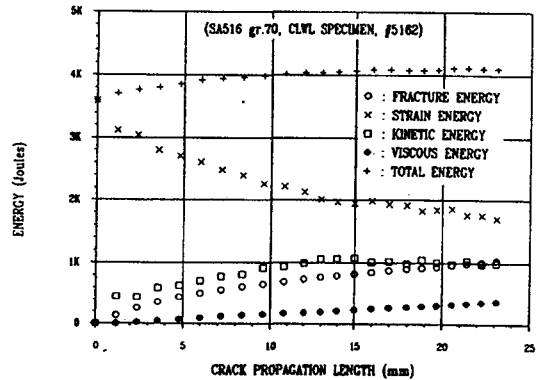
The following are the analysis results by the dynamic crack analysis program (INSAMCR) for the specimens of SA 508 C13 with a thickness of 20mm and SA516 gr.70 with a thickness of 19mm.

3.1 Energies with dynamic crack propagation distance.

Figure 5 shows the change of various energies corresponding to dynamic crack propagation distance. The dynamic crack propagation distance was obtained by using the dynamic propagation velocity as input data. The propagation velocity was computed from the dynamic crack propagation data which were obtained by the crack propagation velocity-measuring equipment (developed for this experiment). At the early stage, the fracture energy of the specimen tends to increase linearly with the dynamic crack propagation while the strain energy tends to decrease linearly. Total energy almost remains constant during the crack propagation, which assures the reliability of our



(a)



(b)

Fig. 5 Calculated Strain, Fracture, Kinetic, Viscous and Total Energy as a Function of Crack Propagation Length

dynamic finite element method and procedure with dynamic crack propagation data as inputs.

The absolute magnitudes of energy are different. However, the changing patterns of the energy are similar to the crack propagation length. The effect of strain energy is dominant at the early stage, but the effect of fracture and kinetic energies becomes larger at the later stage.

3-2 Dynamic Stress Intensity Factor and Dynamic Crack Propagation Distance with Crack Propagation Time

Figure 6 shows dynamic stress intensity factor

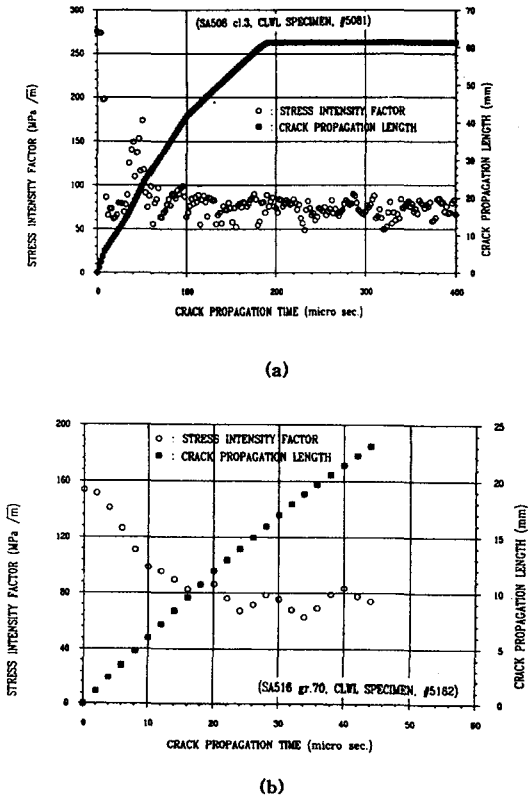


Fig. 6 Extracted Values of Dynamic Stress Intensity Factor and Dynamic Crack Propagation Length as a Function of time

and dynamic crack propagation distance with crack propagation time which were obtained by using INSAMCR.

Figure 6(a) is for the CLWL specimen of SA 508 Cl.3 forged steel which has been used for nuclear pressure vessels of Young Kwang nuclear power plants in Korea. Crack propagation stopped after crack propagates 62mm over about 190μsec through deceleration and acceleration. Initial stress intensity factor of crack has a relatively high value of 275MPa \sqrt{m} and is not constant. It seemed to be effected by machining conditions and loading conditions. Dynamic stress intensity factor decreases rapidly at the initial stage and then tends to decrease slowly with a stress intensity factor (crack arrest toughness) of 76MPa \sqrt{m} .

This tendency indicates that the crack arrest toughness of 76MPa \sqrt{m} can be regarded as a physical quantity characterizing material property. From many experiments we also notice that as the crack propagation length became shorter, the difference between the dynamic and static crack arrest toughnesses decreased. Figure 6(b) is for a SA 516 gr. 70 CLWL specimen with a thickness of 19mm which has tendency similar to that in Fig.6(a). Crack arrest toughness is about 72MPa \sqrt{m} .

3.3 Relationship between Dynamic Stress Intensity Factor and Dynamic Crack Propagation Velocity

Figure 7 shows the relationship between dynamic stress intensity factor and dynamic crack propagation velocity. The data in Fig.7 were

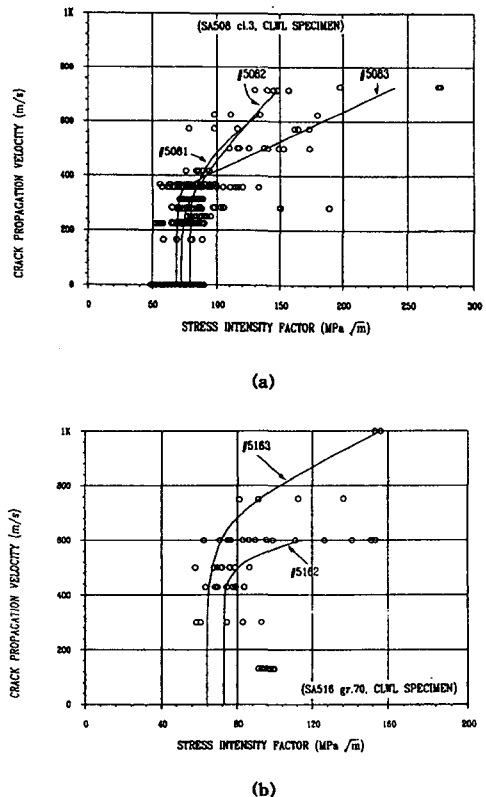


Fig. 7 Relationship between Dynamic Stress Intensity Factor and Dynamic Crack Propagation Velocity

obtained by using INSAMCR program.

It is shown that although the dynamic crack propagation velocity remains constant, the dynamic stress intensity factor changes.

When the scattered data are also taken into account, the relationship between dynamic crack propagation velocity and dynamic fracture toughness may be represented by the typical " I'' " shape curve from which dynamic crack arrest toughness is obtained as in Table 3.

Round-Robin Test results for A533B⁽⁹⁾ are also included in Table 3 for reference.

Table 3. Dynamic Crack Arrest Toughnesses
(experimental temperature : 0-24°C)

Direction of Test	Testing Materials	Dynamic crack arrest toughness (MPa√m)
Nuclear Pressure Vessel Steels	SA508 cl.3	76 ± 20
	SA516 gr.70	72 ± 15
Round-Robin Test(U.S.A)	A533B (10°C)	78.2 ± 9.7
	(25°C)	83.4 ± 10.6

3.4 Empirical Equation Correlating Dynamic Stress Intensity Factor with Dynamic Crack Propagation Velocity.

Using Fig.7 and the averaging of data from many experiments, we obtained following empirical equations correlating dynamic stress intensity factor ($K(\dot{a})$) with dynamic crack propagation velocity (\dot{a}) for nuclear pressure vessel steels :

(a) SA508 Cl.3 case

$$\dot{a} \leq 340 \text{ m/s ,}$$

$$K(\dot{a}) = 76 \pm 20 (\text{MPa}\sqrt{\text{m}})$$

$$\dot{a} \geq 340 \text{ m/s ,}$$

$$K(\dot{a}) = 41.7 \text{Exp}\{0.00177 \dot{a}\} \pm 20 (\text{MPa}\sqrt{\text{m}})$$

(b) SA516 gr.70 case

$$\dot{a} \leq 450 \text{ m/s ,}$$

$$K(\dot{a}) = 72 \pm 15 (\text{MPa}\sqrt{\text{m}})$$

$$\dot{a} \geq 450 \text{ m/s ,}$$

$$K(\dot{a}) = 27.9 \text{Exp}\{0.0028 \dot{a}\} \pm 15 (\text{MPa}\sqrt{\text{m}})$$

4. Conclusion

We determined properly the dynamic stress intensity factor and identified the physical quantities affecting the factor by using INSAMCR(a two-dimensional finite element program for dynamic fracture analysis) and the measuring system for dynamic fracture toughness in the dynamic crack propagation experiments.

Total energy almost remains constant during the crack propagation, which assures the reliability of our dynamic finite element method and procedure with dynamic crack propagation data as inputs.

The crack arrest toughness of 76MPa√m can be regarded as a physical quantity characterizing material property.

The relationship between dynamic crack propagation velocity and dynamic fracture toughness may be represented by the typical " I'' " shape curve.

The empirical equations correlating the dynamic stress intensity factor ($K(\dot{a})$) with the dynamic crack propagation velocity(\dot{a}) are also proposed for SA 508 Cl.3 steel and SA 516 gr.70 steel.

REFERENCES

1. O. S. Lee, "About Dynamic Fracture Mechanics," J. of KSME, Vol. 24, No. 6, pp. 452-458, 1984.
2. G. R. Irwin et al., "A Photoelastic Study of Crack Propagation and Arrest," U.S. NRC Report NUREG/CR-0342, Univ. of Maryland, 1977.
3. G. R. Irwin et al., "Photoelastic Studies of Crack Propagation and Arrest in Polymers and 4340 Steel," U.S. NRC Report NUREG/CR-0342, Univ. of Maryland, 1978.
4. W. G. Knauss, K. Ravi-Chander and A. J. Rosakis, "Workshop on Dynamic Fracture," California Institute of Technology, pp. 11-

- 35, 1983.
5. P. B. Crosley and E. J. Riping et al., "Cooperative Test Program on Crack Arrest Toughness Measurements," NUREG/CR-3261, Final Report, 1983.
 6. O. S. Lee and M. K. Han, "Measurement of Dynamic Crack Propagation Velocity in Polymers," Trans. of KSME, Vol. 13, No. 5, 1989.
 7. O. S. Lee and M. K. Han, "Determination of Dynamic Stress Intensity Factor in Polymers," Proc. of KSAE, pp. 90-95, 1990.
 8. O. S. Lee et al., "Dynamic Stress Intensity Factor and Dynamic Crack Propagation Velocity in Polymers," KOSEF Report, KOSEF 901-0910-013-2, 1992.
 9. D. B. Barker et al., "A Method for Determining the Crack Arrest Fracture Toughness of Ferritic Materials," ASTM STP 969, pp. 569-593, 1988.